JB
Journals.ASM.org

Heterologous Expression of *Bartonella* Adhesin A in *Escherichia coli* by Exchange of Trimeric Autotransporter Adhesin Domains Results in Enhanced Adhesion Properties and a Pathogenic Phenotype

Thomas Schmidgen,[a] Patrick O. Kaiser,[a] Wibke Ballhorn,[a] Bettina Franz,[a] Stephan Göttig,[a] Dirk Linke,[b,c] Volkhard A. J. Kempf[a]

Institut für Medizinische Mikrobiologie und Krankenhaushygiene, Klinikum der Goethe-Universität, Frankfurt am Main, Germany[a]; Max-Planck-Institut für Entwicklungsbiologie, Abteilung Proteinevolution, Tübingen, Germany[b]; Department of Biosciences, University of Oslo, Oslo, Norway[c]

Human-pathogenic *Bartonella henselae* causes cat scratch disease and vasculoproliferative disorders. An important pathogenicity factor of *B. henselae* is the trimeric autotransporter adhesin (TAA) *Bartonella* adhesin A (BadA), which is modularly constructed, consisting of a head, a long and repetitive neck-stalk module, and a membrane anchor. BadA is involved in bacterial autoagglutination, binding to extracellular matrix proteins and host cells, and in proangiogenic reprogramming. The slow growth of *B. henselae* and limited tools for genetic manipulation are obstacles for detailed examination of BadA and its domains. Here, we established a recombinant expression system for BadA mutants in *Escherichia coli* allowing functional analysis of particular BadA domains. Using a BadA mutant lacking 21 neck-stalk repeats (BadA HN23), the BadA HN23 signal sequence was exchanged with that of *E. coli* OmpA, and the BadA membrane anchor was additionally replaced with that of *Yersinia* adhesin A (YadA). Constructs were cloned in *E. coli*, and hybrid protein expression was detected by immunoblotting, fluorescence microscopy, and flow cytometry. Functional analysis revealed that BadA hybrid proteins mediate autoagglutination and binding to collagen and endothelial cells. *In vivo*, expression of this BadA construct correlated with higher pathogenicity of *E. coli* in a *Galleria mellonella* infection model.

Bartonella henselae is a Gram-negative, facultative-intracellular human pathogen transmitted by bloodsucking arthropods or infected cats. Upon infection, immunocompetent patients suffer from cat scratch disease, a self-limiting local lymphadenopathy. In immunosuppressed patients, *B. henselae* infections can result in tumorous proliferations of endothelial cells (ECs), diseases designated bacillary angiomatosis and peliosis hepatis. Vasculoproliferative entities caused by *B. henselae* infections correlate with the activation of hypoxia inducible factor 1 (HIF-1), the key transcription factor involved in angiogenesis (1) and subsequent secretion of vasculoproliferative cytokines (e.g., vascular endothelial growth factor [VEGF]), both occurring *in vitro* and *in vivo* (2, 3).

Adherence to host tissue is the first and crucial step in bacterial infections. Pathogenic bacteria express adhesins to ensure infection of the host. The best-characterized adhesin of *B. henselae* is *Bartonella* adhesin A (BadA), which is enormous (~240 nm in length; monomer, 328 kDa; trimer, ~1,000 kDa) (4). Expression of BadA is decisive for the adherence of *B. henselae* to ECs and extracellular matrix components (e.g., collagen and fibronectin [Fn]) under static and dynamic conditions (5) and correlates with the activation of HIF-1-regulated secretion of proangiogenic cytokines (2–4). So far, all characterized *Bartonella* species harbor BadA homologues in their genomes (6).

BadA is a representative of the trimeric autotransporter adhesins (TAAs), which are widespread pathogenicity factors among Gram-negative bacteria, e.g., *Escherichia coli* immunoglobulin-binding proteins (Eibs) (7), *Neisseria* adhesin A (NadA) of *Neisseria meningitidis* (8), *Haemophilus influenzae* adhesin (Hia) (9), ubiquitous surface proteins A1 and A2 (UspA1 and UspA2) of *Moraxella catarrhalis* (10), or *Xanthomonas* adhesin A (XadA) from the plant pathogen *Xanthomonas oryzae* (11). The prototypic TAA, *Yersinia* adhesin A (YadA) from *Yersinia enterocolitica*, is constructed modularly with an N-terminal head, a neck, a stalk, and a C-terminal membrane anchor domain, and all TAAs are organized similarly (6, 12).

The N-terminal signal sequence of BadA is followed by the head, which is composed of three subdomains (YadA-like head repeat, Trp ring, and GIN domain with high structural similarities to the corresponding domains from *H. influenzae* adhesin Hia [13]). The BadA head is linked to the anchor by a long and highly repetitive neck-stalk module rich in coiled coils varying significantly in length among different *B. henselae* isolates (14). The modular structure of TAAs suggests a domain-function relationship in which certain domains are responsible for certain biological functions. In fact, a truncated BadA mutant lacking 21 of the neck-stalk repeats exhibited no Fn-binding capacity, whereas other biological functions (e.g., collagen binding, adhesion to ECs, and induction of VEGF secretion) were unaffected (15). Recently, the stalk region was identified to represent the Fn-binding site, and a minimal length of four neck-stalk repeats is crucial for Fn binding (16). Additionally, the function of the *B. henselae* VirB/D4 type 4 secretion system depends on the expression and length of BadA: the longer the BadA construct, the less efficient was the secretion of effector proteins into host cells (17).

Further molecular and functional analysis of the modularly constructed BadA would allow to understand the interaction of TAA domains with their respective binding partners. However,

Received 19 December 2013 **Accepted** 19 March 2014
Published ahead of print 28 March 2014
Address correspondence to Volkhard A. J. Kempf, volkhard.kempf@kgu.de.

doi:10.1128/JB.01461-13

TABLE 1 Bacterial strains used in this study

Strain	Characteristics	Reference(s) or source
B. henselae strain Marseille	Wild type, expressing BadA	4, 51
E. coli DH5α	Host strain used for cloning	Life Technologies
E. coli BL21(DE3) Omp2	Host strain used for expression of BadA HN23 and BadA HN23 hybrids; *ompF*::Tn*5*	22
E. coli BL21(DE3) Omp8	Host strain used for expression of BadA HN23 and BadA HN23 hybrids; Δ*lamB ompF*::Tn*5* Δ*ompA* Δ*ompC*	52
E. coli BL21(DE3) Omp8Δ*degP*	Host strain used for expression of BadA HN23 and BadA HN23 hybrids; Δ*lamB ompF*::Tn*5* Δ*ompA* Δ*ompC* Δ*degP*	52

due to the slow growth of *Bartonella*, phase variation, and difficulties in performing molecular genetics, orthologous expression of modified BadA fibers is challenging. Earlier extensive efforts of our group to express full-length BadA in *E. coli* were not successful (unpublished data), although such expression would facilitate the functional analysis of BadA and its domains.

Here, we modified a truncated BadA mutant lacking 21 neck-stalk repeats (BadA HN23) of the alphaproteobacterium *B. henselae* and altered its composition by exchanging the signal sequence and the membrane anchor domain to that of gammaproteobacteria. Hybrid proteins were expressed on the surface of *E. coli* mediating the biological functions of autoagglutination, collagen and host cell adherence, and, moreover, pathogenicity in an *in vivo* infection model. Our results demonstrate that BadA can be recombinantly expressed in *E. coli* when an autotransporter domain of a gammaproteobacterium is present and, more generally, that certain domains can be swapped between certain TAAs without loss of function, even between bacteria from different subdivisions underlining the concept of modular TAA evolution.

MATERIALS AND METHODS

Bacterial strains and growth conditions. *B. henselae* was grown in a humidified atmosphere at 37°C and 5% CO_2 on Columbia blood agar (CBA). *E. coli* strains used in this study are listed in Table 1. Bacteria were grown at 37°C in Luria-Bertani (LB) broth with the appropriate antibiotics (ampicillin, 100 μg/ml; kanamycin, 50 μg/ml).

***In silico* construction of BadA HN23 hybrids.** Fusion constructs between the YadA membrane anchor and the BadA stalk were designed as follows: annotation of TAA domains was performed using the daTAA analysis tool (18). Coiled-coil analysis of the segments close to the membrane anchor was performed manually, following the example of YadA (19). In short, the YTD motifs reminiscent of the noncanonical 19-residue repeats responsible for a transition from left- to right-handed coiled coil were identified. The constructs were designed such that the final fusion product contains the most C-terminal YTD-YTD element from BadA, replacing the equivalent element of identical length in YadA through an XhoI site introduced by synonymous point mutations into the most C-terminal YTD.

Cloning of *badA* HN23 hybrids. The plasmids and primers used in this study are listed in Table 2 and Table 3. DNA modifications were done according to standard protocols. The fusion construct *badA* HN23 (borne on plasmid pPK3) has been produced as described previously (15). For cloning of *badA* HN23 in pASK-IBA33plus (IBA GmbH, Göttingen, Germany), the *badA* HN23 fragment from plasmid pPK3 (without its putative *B. henselae* promoter sequence) was amplified by PCR using the primers BY3fw and BadAr27, resulting in a 2,136-bp fragment. PCR product and vector were digested with BsaI (Fermentas, St. Leon-Rot, Germany), and the insert was cloned in frame into vector pASK-IBA33plus (IBA), resulting in plasmid pTS4.

For the construction of *badA* HN23 hybrid 1, a *badA* HN23 fragment without the *badA* signal sequence was generated from *badA* HN23 (pPK3) by PCR using the primers BY2fw and BadArev27, generating a 1,994-bp fragment. The PCR product was digested with BsaI and inserted in frame into the BsaI-digested vector pASK-IBA2 (IBA), resulting in plasmid pTS2.

Cloning of *badA* HN23 hybrid 2 and *badA* HN23 hybrid 3 was done in a two-step process. First, the *yadA* membrane anchor sequence (amino acids [aa] 330 to 422, resulting in bp 988 to 1269, referring to NCBI gene sequence EKA25166.1) was amplified using the primers BY1fw and BY1rev from plasmid pUC-A1 (20), generating a 371-bp PCR product. This fragment was digested with XhoI and HindIII (Fermentas) and inserted into pASK-IBA33plus, resulting in plasmid pTS1, or into pASK-IBA2, generating plasmid pTS5. In the second step, a 1,854-bp fragment containing domain *badA* HN23 with signal sequence but without the *badA* membrane anchor sequence was generated by PCR with primers BY3fw and BY2rev from plasmid pPK3. This fragment was inserted via

TABLE 2 Plasmids used in this study

Plasmid	Characteristics	Resistance	Reference or source
pASK-IBA2	AHTC-inducible expression vector containing *ompA* signal sequence	Amp^r	IBA GmbH
pASK-IBA33plus	AHTC-inducible expression vector without *ompA* signal sequence	Amp^r	IBA GmbH
pPK3	pCR-Blunt II TOPO with 3.1-kb BadA HN23 insert	Km^r	15
pUC-A1	pUC13 containing *yadA* gene	Amp^r	20
pTS1	pASK-IBA33plus containing *yadA* membrane anchor sequence	Amp^r	This study
pTS2 (hybrid 1)	pASK-IBA2 containing *ompA* signal sequence-*badA* HN23-*badA* membrane anchor construct	Amp^r	This study
pTS3 (hybrid 2)	pASK-IBA33plus containing *badA* signal sequence-*badA* HN23-*yadA* membrane anchor construct	Amp^r	This study
pTS4	pASK-IBA33plus containing BadA HN23	Amp^r	This study
pTS5	pASK-IBA2 containing *yadA* membrane anchor sequence	Amp^r	This study
pPK5 (hybrid 3)	pASK-IBA2 containing *ompA* signal sequence-*badA* HN23-*yadA* membrane anchor construct	Amp^r	This study

TABLE 3 Primers used in this study[a]

Primer	Sequence (5′→3′)
BY1fw	GGATCCCTCGAGGTCGACCTGCAGGGGGACCATGGTCTCATA CACAGATCATAAATTCCGTCAACTTG
BY1rev	CAGGTCAAGCTTATTACCACTCGATATTAAATGATGCATTG
BY2fw	CATCTCGGTCTCCGGCCTCGAATCTTGCGCTTACAGGAG
BY2rev	CAGGTCAAGCTTATTACCACTCGATATTAAATGATGCATTG
BY3fw	CATCTCGGTCTCCAATGAAAAAATTATCTGTCACATCAAAGAGAC
BadArev27	AATATGGTCTCTGCGCTCATTTCAGTCTCAAAGTAATCCCTG

[a] All primers were designed in this study.

BsaI into the vector pTS1, creating the plasmid pTS3, which contains *badA* HN23 hybrid 2. The cloning of *badA* HN23 hybrid 3 was performed in a similar way. Here, a 1,714-bp fragment consisting of *badA* HN23 without the *badA* signal sequence and *badA* membrane anchor sequence was inserted via BsaI restriction sites into plasmid pTS5, resulting in plasmid pPK5.

Heterologous expression of BadA HN23 and BadA HN23 hybrids in *E. coli*. For expression of BadA HN23 and BadA HN23 hybrids in *E. coli* BL21(DE3) Omp2, *E. coli* BL21(DE3) Omp8, and *E. coli* BL21(DE3) Omp8Δ*degP*, an overnight culture of the respective expression plasmid-carrying strain was diluted 1:10 in LB medium (supplemented with appropriate antibiotics) and grown to an optical density at 600 nm (OD_{600}) of 0.5. Gene expression was induced for 30 min at 37°C by addition of 40 ng/ml anhydrotetracyclin (AHTC; IBA GmbH, Göttingen, Germany).

Immunofluorescence microscopy. The expression of BadA HN23 and BadA HN23 hybrids 1 to 3 on the bacterial cell surface was assessed by immunostaining with a Bad HN23-specific antibody (4, 15). Gene expression was induced as described above. Subsequently, bacteria were washed and resuspended in phosphate-buffered saline (PBS). Bacterial suspensions (30 μl each) were spotted onto glass slides, air dried, and fixed with 3.75% PBS-buffered paraformaldehyde (PFA) for 15 min at 4°C. PFA-fixed bacteria were washed three times with PBS at the beginning and after each incubation step. Incubation with the primary antibody (rabbit IgG) was done for 60 min at room temperature (RT) followed by incubation with a carbocyanine (Cy2)-conjugated secondary anti-IgG antibody (Dianova, Hamburg, Germany) for 45 min. Bacterial DNA was counterstained with 1 μg/ml of 4′,6-diamidino-2-phenylindole (DAPI) for 5 min at 5°C. Finally, slides were mounted with Fluoprep medium (bioMérieux, Nürtingen, Germany) and analyzed with a Zeiss Axio Imager M.2 microscope (Zeiss, Jena, Germany) equipped with a Visitron monochromatic digital camera and the related Visiview software (Visitron, Puchheim, Germany).

SDS-PAGE and immunoblotting. Gene expression was induced as described above. *E. coli* cells were resuspended in sodium dodecyl sulfate (SDS) sample buffer and heated at 95°C for 5 min. SDS-polyacrylamide gel electropheresis (PAGE) was performed using 12% gels. For immunoblotting, proteins were transferred onto nitrocellulose membranes (Schleicher & Schüll, Dassel, Germany). Blots were blocked for 1 h using 5% skim milk powder, resuspended in 25 mM Tris (pH 7.5), 0.15 M NaCl, and 0.05% Tween 20 (Sigma-Aldrich, Deisenhofen, Germany), and incubated with anti-BadA rabbit IgG (1:2,000 diluted in skim milk) overnight. Bound primary antibodies were detected by peroxidase-conjugated anti-rabbit IgG antibodies (1:1,000; Dako, Glostrup, Denmark). Signals were visualized by chemiluminescence (GE Healthcare, Freiburg, Germany).

Quantification of BadA HN23 surface expression. For quantification of BadA HN23 surface expression, gene expression was induced as described above, and 1.0×10^9 bacteria were harvested by centrifugation. Cells were washed with PBS, fixed with 4% PFA, and washed again. Bacteria were stained with a rabbit anti-BadA antibody (1:200; 1 h at RT), which was also used for Western blot and immunofluorescence analysis. After washing, cells were stained with an Alexa Fluor 488-conjugated secondary antibody (1:100; Dianova) and washed again. Surface expression was analyzed using a FACSCalibur flow cytometer (Becton, Dickinson, Heidelberg, Germany), and data were subsequently quantified using FlowJo (Tree Star Inc., Ashland, OR, USA).

Autoagglutination assay. Gene expression in *E. coli* BL21(DE3) Omp2/BadA HN23 hybrid 3 was induced as described above. Autoagglutination was assayed macroscopically according to the method of Laird and Cavanaugh (21). Suspensions containing 2.0×10^9 bacteria/ml (resuspended in PBS) were incubated for 1 h at RT in transparent plastic tubes. Clearance of the suspension was recorded with a digital camera (Nikon D3100; Düsseldorf, Germany).

For microscopic analysis of autoagglutination, 2.0×10^9 bacteria were resuspended in 1 ml PBS and transferred into a transparent plastic tube. After 1 h of incubation at RT, 30 μl of the suspension was taken from the middle of the tube, spotted onto a glass slide, air dried, and fixed with 3.75% PFA. After washing with PBS, bacteria were stained with DAPI. Autoagglutination was evaluated by fluorescence microscopy as described above.

Determination of collagen binding of *E. coli* BL21(DE3) Omp2/BadA HN23 hybrid 3. To determine the ability of the BadA HN23 hybrid 3-expressing *E. coli* BL21(DE3) Omp2 strain (22) to bind to collagen, gene expression was induced as described above. Coverslips were coated with 1 ml of collagen G (Biochrom, Berlin, Germany) at a concentration of 10 μg/ml (diluted in PBS) for 24 h at RT. Bacteria were adjusted to 2.0×10^8 cells/ml and sedimented on coverslips by centrifugation ($300 \times g$, 5 min). After 30 min of incubation at 37°C, coverslips were washed three times thoroughly with PBS and fixed with 3.75% PFA, and adherent bacteria were stained with DAPI. Adherence was analyzed by fluorescence microscopy. Bacterial adherence was quantified by counting the pixels gained by the fluorescent bacteria from 60 independent microscopic fields (3×20) from three different coverslips using the ImageJ software (http://rsb.info.nih.gov/ij/index.html).

Adherence to endothelial cells. Human umbilical vein endothelial cells (HUVECs), obtained with ethics permission 4/12 of the Frankfurt University Hospital ethics committee, were cultured in endothelial cell growth medium (PromoCell, Heidelberg, Germany) as described previously (23). For adherence assays, 1.0×10^5 cells were seeded into collagen G-coated wells in a 24-well plate, grown overnight without antibiotics, and infected with 1.0×10^7 *E. coli* cells by centrifugation (multiplicity of infection [MOI], 100; $300 \times g$, 5 min). Cells were incubated for 15 min in a humidified atmosphere at 37°C and 5% CO_2. Samples were washed three times with prewarmed cell culture medium to remove nonadherent bacteria, and total adherent bacteria were quantified by osmotic cell lysis as described previously (23). For this purpose, HUVECs were lysed by adding 900 μl sterile deionized water per well. After 4 min of incubation at RT, lysis was controlled microscopically and stopped by adding 100 μl 10× PBS. Serial dilutions were plated on Mueller-Hinton agar plates, and adherent bacteria were quantified by counting the CFU. The percentage of cell-adherent bacteria was calculated as the ratio of adherent bacteria to the bacterial inoculum.

***G. mellonella* infection model.** The larvae of the greater wax moth (*Galleria mellonella*) were used as an *in vivo* model to examine the pathogenicity of *E. coli* Omp2 expressing Bad HN23 hybrid 3 in contrast to the empty vector control. *G. mellonella* larvae were purchased from suppliers (Terraristika Express, Recklinghausen, Germany) and were stored no longer than 7 days upon delivery at 4°C in the dark. Two larvae of each batch were homogenized in PBS, and serial dilutions were plated on Columbia blood agar plates supplemented with 5% sheep blood (Becton, Dickinson) to exclude contaminations of larvae with Gram-negative or insectopathogenic bacteria species (e.g., *Klebsiella pneumoniae*, *Pseudomonas aeruginosa*, or *Proteus* spp.). Noncontaminated batches of larvae were chosen for infection experiments as described earlier (24).

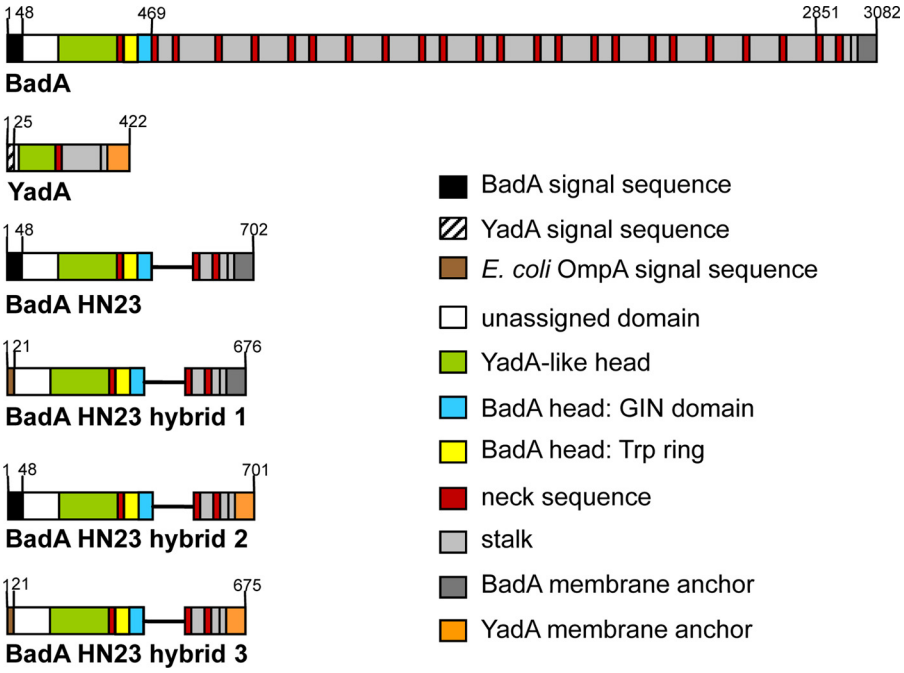

FIG 1 Schematic diagram and domain organization of BadA of *B. henselae* Marseille and YadA of *Y. enterocolitica* (strain WA-314), truncated BadA (BadA HN23 [15]) and BadA HN23 hybrid constructs. BadA hybrid 1 has been constructed by replacing the BadA signal sequence (aa 1 to 48) with that of OmpA from *E. coli* ATCC 700926 K-12 substrain MG1655. BadA hybrid 2 was generated by replacing the BadA membrane anchor with that of YadA (aa 330 to 422). BadA hybrid 3 has been constructed by replacing both the BadA signal sequence with that of OmpA and the BadA membrane anchor with that of YadA. Domains were annotated using the daTAA tool (18) and drawn to scale (according to sequence length).

Gene expression in *E. coli* was induced as described above. Bacteria (1.0×10^7) were resuspended in 10 μl sterile PBS and injected into the hemocoel via the last left proleg of the larvae using a Hamilton syringe. In total, 30 larvae were infected with each strain. Control larvae ($n = 30$) were inoculated with 10 μl PBS to exclude that an injection trauma might affect survival of the larvae. Larvae were stored in petri dishes at 37°C for 120 h and scored for survival daily. Larvae were considered dead if they failed to respond to touch as described previously (24).

Expression of BadA HN23 hybrid 3 was evaluated 1 day postinfection by BadA immunofluorescence staining (see above) of *E. coli* reisolated from larva homogenates cultivated on ampicillin- and kanamycin-containing Mueller-Hinton agar plates for 24 h.

Statistical analysis. All experiments were performed at least three times and revealed comparable results. Differences between mean values of experimental and control groups were analyzed by Student's *t* test. A *P* value of <0.01 was considered statistically significant. Survival curves of *G. mellonella* were generated using Kaplan-Meier survival estimates. Log rank tests were performed to compare differences of survival curves. A *P* value of <0.05 was considered statistically significant (Prism4; Graphpad Software, San Diego, CA, USA).

RESULTS

Cloning of *badA* HN23 and *badA* HN23 hybrids in *E. coli*. In order to establish an expression system for BadA mutants in *E. coli*, a BadA mutant sequence lacking 21 neck/stalk repeats (BadA HN23) was cloned into AHTC-inducible expression vectors. *badA* HN23 hybrid proteins (hybrids 1 to 3) were created either by the exchange of the *badA* signal sequence with that of *E. coli ompA* (hybrid 1) or by the exchange of the *badA* membrane anchor sequence with that of *yadA* (hybrid 2) or both (hybrid 3) (Fig. 1).

badA HN23 (including the BadA signal sequence) was cloned in *E. coli* by amplifying the whole gene from pPK3, and insertion into the AHTC-inducible vector pASK-IBA33plus was performed via BsaI receiving plasmid pTS4. Hybrid 1 was created by inserting the *badA* HN23 sequence without its signal sequence into pASK-IBA2, resulting in plasmid pTS2. This expression vector contained the *ompA* signal sequence for protein transport into the periplasm, generating an *ompA-badA* HN23 construct. Hybrid 2 was generated by the fusion of *badA* HN23 (including the *badA* signal sequence but lacking the *badA* membrane anchor sequence) with the *yadA* membrane anchor sequence previously inserted in pASK-IBA33plus (pTS1), resulting in plasmid pTS3. Hybrid 3 was constructed by the fusion of *badA* HN23 (*badA* signal sequence replaced by *ompA* signal sequence and lacking the *badA* membrane anchor sequence) with the *yadA* membrane anchor sequence previously inserted in pASK-IBA2 (denoted pTS5), resulting in plasmid pPK5.

Heterologous expression of BadA HN23 and BadA HN23 hybrids in *E. coli*. To assess if BadA HN23 and BadA HN23 hybrids are heterologously expressed, protein expression was induced by the addition of AHTC to liquid culture for 30 min, and expression was controlled by fluorescence microscopy. Gene induction resulted in a strong surface expression displaying as specific circular, rod-shaped fluorescence signals ("halo" phenomenon) in the expression strains [*E. coli* BL21(DE3) Omp8; hybrid 3; Fig. 2A]. A weaker fluorescence signal was observed for BadA HN23 hybrids 1 and 2 and BadA HN23 when using *E. coli* BL21(DE3) Omp8 and *E. coli* BL21(DE3) Omp8Δ*degP* (data not shown). Protein expression was further analyzed by immunoblotting. Results demonstrated that all four constructs (BadA HN23 hybrids 1 to 3 and BadA HN23) were synthesized in the respective AHTC-induced bacteria, while noninduced samples showed no specific protein

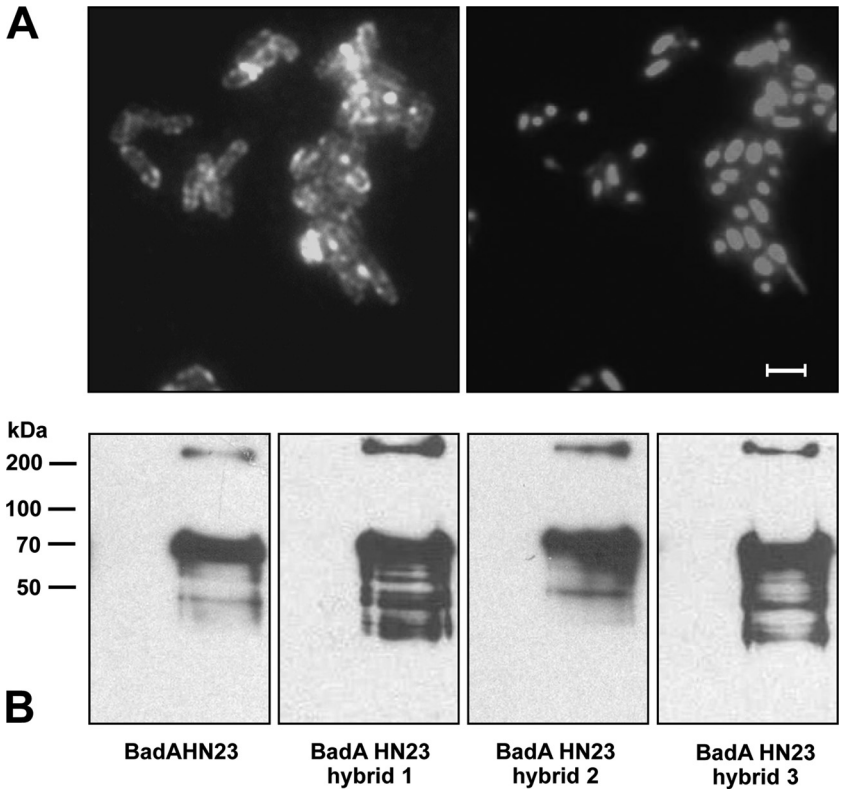

FIG 2 Heterologous BadA HN23 and BadA HN23 hybrid expression in *E. coli* BL21(DE3) Omp8. (A) Detection of BadA hybrid 3 protein surface expression by immunofluorescence using anti-BadA specific antibodies (left). Note the halo phenomenon indicating surface expression. For control, bacteria were stained with DAPI (right). Scale bar, 2 μm. (B) Detection of BadA constructs by immunoblotting. Expression of BadA HN23, BadA HN23 hybrids 1 to 3 (hybrids 1 and 3, ~69 kDa; hybrid 2, ~73 kDa) and the corresponding trimers (all, ~210 kDa) was detected by SDS-PAGE and immunoblotting using anti-BadA specific antibodies. Cell lysates from noninduced bacteria were used as negative controls.

bands. Under denaturing conditions, the samples contained mostly the monomeric form of BadA HN23 and BadA HN23 hybrids 1 to 3 (BadA HN23 and hybrid 2, 73 kDa; hybrids 1 and 3, 69 kDa); however, trimers (~210 kDa) were also detectable (Fig. 2B). Flow cytometric analysis revealed that *E. coli* strain Omp2 BadA HN23 hybrid 2 (mean fluorescence intensity [MFI], 71.9) and *E. coli* BadA HN23 hybrid 3 (MFI, 54.7) exhibited a similar surface expression level, which was much less in *E. coli* Omp2 BadA HN23 (MFI, 4.8) and BadA HN23 hybrid 1 (MFI, 3.4); the MFI in the negative control was 1.8 (Fig. 3). Additionally, as BadA hybrid 3-expressing *E. coli* BL21(DE3) Omp8 and *E. coli* BL21(DE3) Omp8Δ*degP* showed a significantly reduced growth rate (data not shown), further experiments were performed using *E. coli* BL21(DE3) Omp2. BadA HN23 hybrid 3 was chosen for further experiments because of its intense and homogeneously distributed fluorescent signal on the bacterial surface. In summary, these data demonstrate that heterologous expression of BadA constructs in *E. coli* is technically possible and that proper autotransporter function of the BadA constructs is an indispensable prerequisite for further functional experiments.

Autoagglutination of *E. coli* mediated by BadA HN23 hybrid 3. Typically, TAAs mediate autoagglutination, and this has been shown for BadA of *B. henselae* (4, 14), the variable outer membrane proteins (Vomps) of *Bartonella quintana* (25), YadA of *Y. enterocolitica*, and EibD of *E. coli* (26, 27). Additionally, BadA HN23 was described earlier to mediate autoagglutination of *B. henselae* (15). Therefore, the ability of BadA HN23 hybrid 3 to confer autoagglutination of *E. coli* was analyzed. For this purpose, BadA HN23 hybrid 3-expressing *E. coli* cells were incubated in PBS in transparent plastic tubes and autoagglutination was evaluated by the method of Laird and Cavanaugh (21). Here, a suspension with *E. coli* BadA HN23 hybrid 3 showed rapid clearance by sedimentation of bacterial aggregates, whereas the control suspension remained turbid (Fig. 4A). In addition, fluorescence microscopy analysis demonstrated that expression of hybrid 3 resulted in the formation of dense aggregates, and this phenomenon was not detectable in control bacteria, which appeared to be spread in the microscopic field as single, nonattaching cells (Fig. 4B). From this, we conclude that heterologous BadA HN23 hybrid protein expression results in autoagglutination very similar to what has been described for *B. henselae*.

Adherence of *E. coli* BL21(DE3) Omp2/BadA HN23 hybrid 3 to collagen. TAAs bind to extracellular matrix components, and BadA was shown to mediate, e.g., the adherence of *B. henselae* to collagens I, III, and IV (5, 12). Truncated BadA HN23 is sufficient for collagen binding (15). To analyze whether this biological function can be transferred to *E. coli* expressing BadA HN23, bacteria were exposed to collagen G-coated coverslips and adherence was analyzed by DAPI staining and subsequent fluorescence microscopy.

Results displayed that BadA HN23 hybrid 3-expressing *E. coli* showed a significantly higher binding to collagen-coated coverslips than that obtained with the *E. coli* vector control (Fig. 5A).

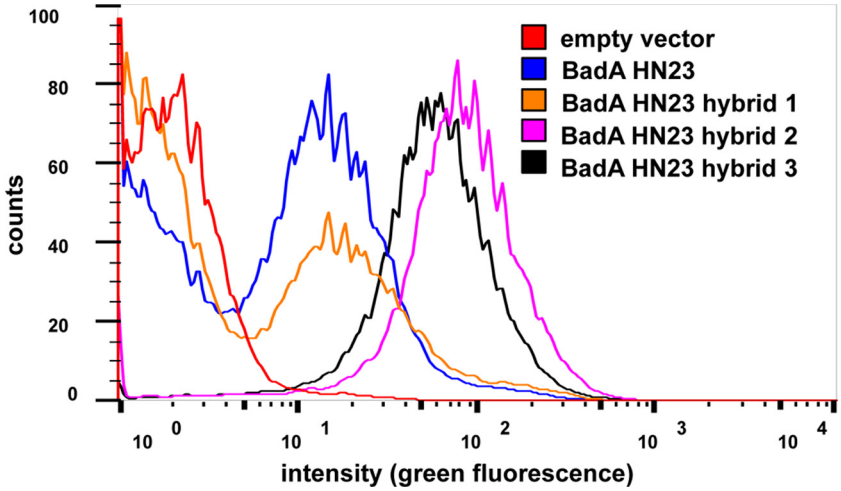

FIG 3 Flow cytometry analysis of *E. coli* expressing BadA HN23 and hybrid proteins 1 to 3. Gene expression was induced as described in Materials and Methods. BadA hybrid protein surface expression was detected using anti-BadA and Alexa Fluor 488-conjugated secondary antibodies. *E. coli* (empty vector control) served as negative control. Mean fluorescence intensities were calculated using FlowJo software.

Again, a strong autoagglutination phenotype was observed. *E. coli* BadA HN23 hybrid 3 showed a ~20-fold-higher adherence to collagen than the respective negative-control strain as determined by semiautomated quantitative image analysis (Fig. 5B).

Adherence of *E. coli* BL21(DE3) Omp2/BadA HN23 hybrid 3 to endothelial cells. Endothelial cells (ECs) represent one of the major targets for the endotheliotropic pathogen *B. henselae* (6). A crucial role of *B. henselae* BadA in the infection process of ECs was demonstrated (4), and the head domain of BadA turned out to be decisive for EC binding (15). However, *B. henselae* harbors further potential adhesins in its genome, e.g., filamentous hemagglutinins (17, 28), which might interact with this process. Therefore, we investigated BadA-mediated adherence to ECs using *E. coli* expressing BadA HN23 hybrid 3. To minimize toxic effects on ECs caused by *E. coli*, the time of infection was reduced to 15 min, since longer infection periods led to cell death (data not shown). In contrast to what was seen in control bacteria (*E. coli* empty vector control), expression of BadA HN23 hybrid 3 resulted in a ~4-fold-higher adherence to ECs, indicating that the expression of BadA HN23 hybrid 3 is sufficient to mediate host cell binding (Fig. 6). Therefore, recombinant expression of truncated BadA from the alphaproteobacterium *B. henselae* mediates three of the typical biological BadA functions when expressed by the gammaproteobacterium *E. coli* (autoagglutination, collagen binding, and EC binding).

Pathogenicity of *E. coli* BL21(DE3) Omp2/BadA HN23 hybrid 3 in *Galleria mellonella*. To evaluate whether expression of BadA HN23 might contribute *in vitro* not exclusively to various adhesion phenotypes of *E. coli* but also to possible pathogenicity, we employed an *in vivo* infection model using larvae of *G. mellonella*. Larvae were injected either with *E. coli* (empty vector control) or with *E. coli* expressing BadA HN23 hybrid 3 and were monitored over a period of 5 days (Fig. 7). Infection of larvae with *E. coli* BadA HN23 hybrid 3 showed a significantly lower ($P < 0.01$) survival rate of 23.3%, whereas infection with the respective negative-control strain resulted in a survival of 46.6%. For control reasons, BadA HN23 hybrid 3 expression of the inoculated bacteria was proven by immunofluorescence staining of reisolated bacteria showing growth on the appropriate selection media (containing kanamycin and ampicillin) and a clear BadA HN23-specific immunofluorescence signal excluding the loss of the plasmid (data not shown). These results demonstrate that expressing BadA HN23 hybrid 3 in *E. coli* doubles infection mortality in *G. mellonella* larvae and argue strongly for a crucial role in pathogenicity.

DISCUSSION

TAAs represent an important group of pathogenicity factors among Gram-negative bacteria. All TAAs are modularly assembled and constructed of head, neck, stalk, and membrane anchor elements. The autotransporter function is determined by the C-terminal membrane anchor domain (12). The conserved modular composition of TAAs suggests a correlation between single TAA domains and one or more distinct biological functions, and this might indicate protein evolution by domain composition and domain exchange.

For the prototypic TAA YadA, it was demonstrated that the head domain mediates binding to ECM proteins (e.g., collagen) and several host cell types (29–32) while the region mediating serum resistance is still unknown. It was observed that an exchange of the YadA membrane anchor domain with that of Hia, EibA, or UspA1 from other gammaproteobacteria leads to comparable surface expression of such chimeric YadA proteins in *Y. enterocolitica* whereas virulence of these chimeric-protein-expressing strains was reduced for unclear reasons compared to wild-type YadA-expressing *Y. enterocolitica* (20). Accordingly, the exact locus of YadA mediating complement resistance of *Y. enterocolitica* by C3b and subsequent factor H binding could not be assigned in a recent study (33).

So far, BadA is the longest characterized member of the TAA family. First attempts at domain-function analysis have been performed by expressing truncated mutant forms of BadA in *B. henselae*. This mutant was lacking 21 of 23 neck-stalk repeats (BadA HN23) and was still capable of mediating autoagglutination, binding to collagen and ECs, and inducing VEGF secretion, whereas the Fn-binding capacity was lost (15). Thus, Fn binding was attributed to the BadA stalk region. A minimal length of four

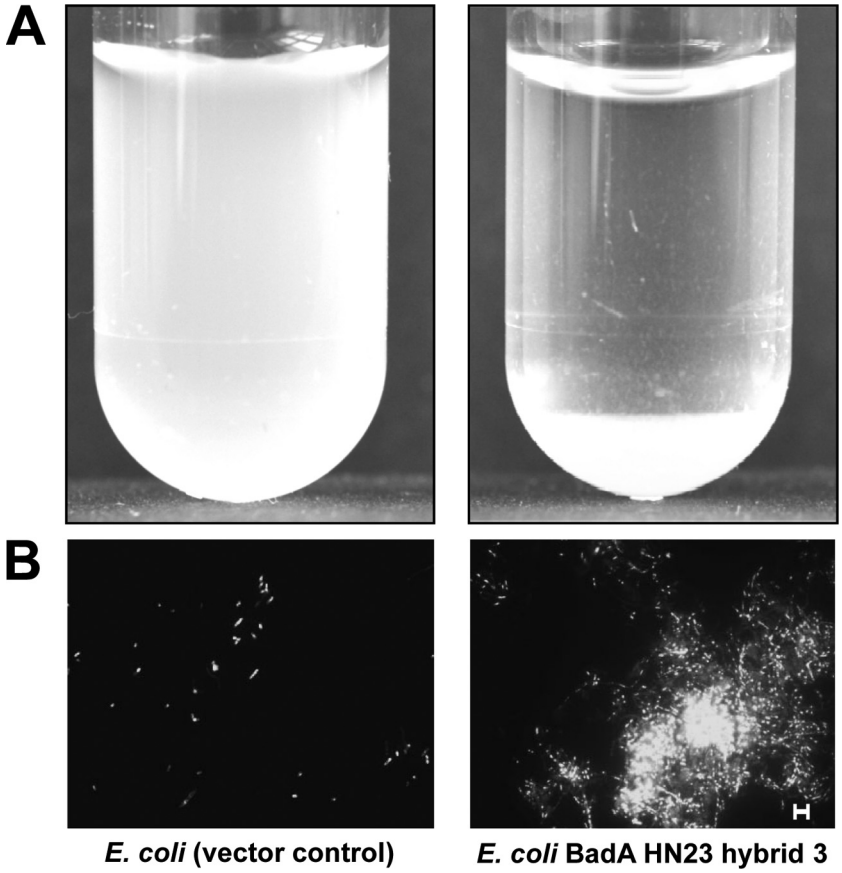

FIG 4 Autoagglutination of BadA HN23-expressing *E. coli*. (A) Macroscopic determination by clearance of bacterial suspensions as a qualitative indicator of autoagglutination. Bacteria were resuspended in PBS, transferred to a transparent plastic tube, and incubated for 1 h at RT. Note the clearance and pellet formation (bottom of tube) in BadA HN23 hybrid 3-expressing *E. coli*, which does not occur in the *E. coli* vector control. (B) Analysis of autoagglutination by fluorescence microscopy. After 1 h of incubation at room temperature, bacteria were spotted onto a glass slide and stained with DAPI. Note the vector control containing single bacterial cells and BadA HN23 hybrid 3-expressing *E. coli* forming dense cell aggregates. Scale bar, 5 μm.

neck-stalk repeats is necessary (16), and attempts to map the exact locus of Fn binding are ongoing. Surprisingly, and in contrast to what occurs in *Y. enterocolitica*, where YadA enhances type III secretion of *Yersinia* outer proteins into host cells (34), injection of *Bartonella* effector proteins (Beps) into host cells by the *B. henselae* VirB/D4 type 4 secretion system is inhibited by BadA expression (17). However, it has to be emphasized that functional analysis of single BadA domains by orthologous expression in *B. henselae* is complicated by the limited number of genetic tools for construction of such mutants and the very slow growth of the pathogen (6). Additionally, *B. henselae* possesses several further adhesin molecules (e.g., filamentous hemagglutinins [28]), which potentially mask the loss of BadA-mediated biological functions. Therefore, a "clean" heterologous expression system for BadA or BadA mutants should be useful in many respects.

Since the first description of BadA in 2004 (4), we and others never have been able to express full-length BadA in *E. coli*. This failure might have been caused by several reasons: (i) the enormous size of *badA* (9.3 kb) possibly affecting cloning procedures and the size of the BadA protein (monomer, 340 kDa), which might hinder correct protein folding, protein transport, and thereby, recombinant expression; (ii) the use of expression strains deficient for chaperones, affecting protein assembly; or (iii) a more general impaired capability to express proteins of alphaproteobacteria (here, *B. henselae*) in gammaproteobacteria (here, *E. coli*). To overcome these problems, we used here a truncated version of BadA (construct size, ~2,000 bp, hybrids 1 and 3, 69 kDa; hybrid 2, 73 kDa) expressed in *E. coli*. Moreover, it has recently been described that assembly and expression of YadA in *E. coli* depend on the presence of BamA, which might act as a chaperone recognizing the C terminus of YadA, although the exact mode of interaction remains unclear (35). The presence of *bamA* has been described *in silico* for *B. henselae* (36), and it was shown that the protein contains five polypeptide transport-associated (POTRA) domains just as BamA from *E. coli*: gi|49475450|ref|YP_8 033491.1|, gi|49475496|ref|YP_033537.1|, gi|49475561|ref|YP_ 033602.1|, gi|49475440|ref|YP_033481.1| (all hemolysin activator protein Hec, part of two-partner secretion system), gi|49475416|ref|YP_ 033457.1| outer membrane protein (BamA/Omp85). The mechanism for the recognition of outer membrane beta-barrel proteins (OMPs) by the Bam complex is not fully resolved, but it seems that a C-terminal OMP motif plays a major role and has some species specificity. While this specificity largely overlaps different bacterial species, individual sequences might not be recognized in heterologous expression systems (37). Whether and how BamA (mis-)recognition might interfere with BadA expression in *E. coli* need to be elucidated in future.

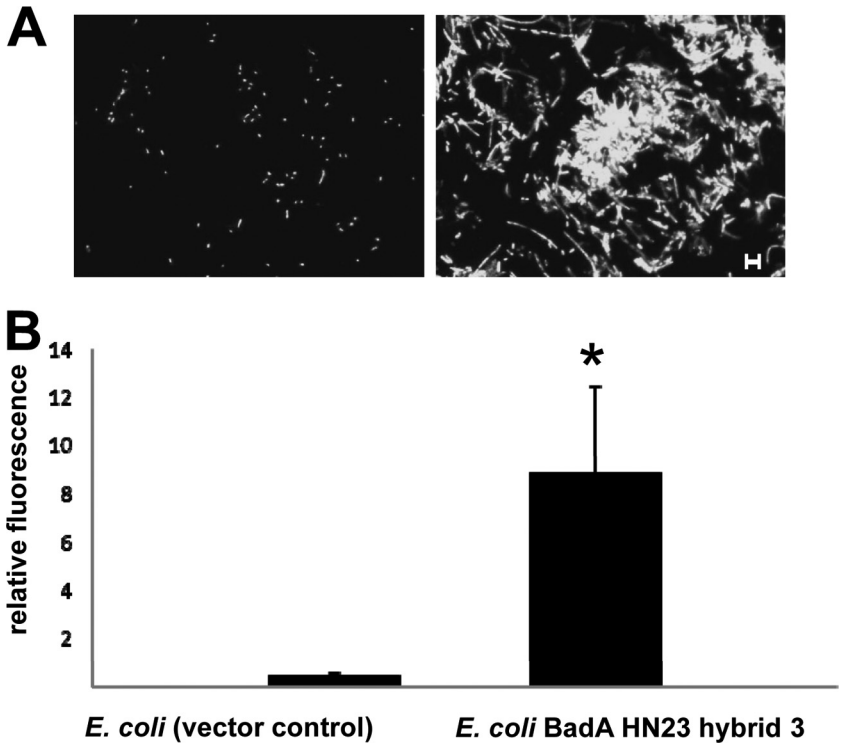

FIG 5 Binding of BadA HN23-expressing *E. coli* to collagen. (A) Collagen G-coated coverslips were incubated with 2.0×10^8 bacteria, washed, stained with DAPI, and analyzed by fluorescence microscopy. Note the significantly increased collagen binding of BadA HN23 hybrid 3-expressing *E. coli* compared to the vector control. Scale bar, 5 μm. (B) Quantitative analysis of collagen-binding bacteria. Sixty independent microscopic fields were quantified by counting the pixels of fluorescent bacteria using the ImageJ software (relative fluorescence). *, significant difference ($P < 0.01$).

The strongest surface expression of BadA HN23 was observed by immunofluorescence microscopy when BadA HN23 hybrid 3 was expressed in *E. coli* (Fig. 2A), and comparable expression was confirmed using flow cytometric analysis (Fig. 3), suggesting that the exchange of the BadA HN23 membrane anchor to that of YadA seems to increase the autotransport activity of the hybrid protein. Immunoblotting revealed that BadA HN23 and all the BadA HN23 hybrid constructs are produced upon gene induction.

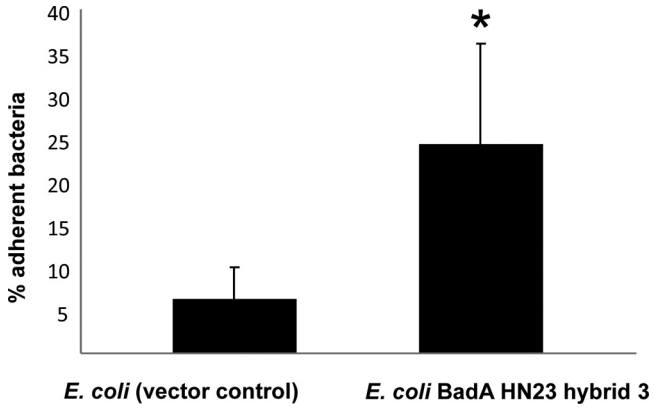

FIG 6 Adhesion of BadA HN23-expressing *E. coli* to endothelial cells. HUVECs (1.0×10^5) were seeded into 24-well plates overnight and exposed to 1.0×10^7 bacteria (MOI, 100) for 15 min. After washing and cell lysis, adherent bacteria were quantified by counting CFU plated in logarithmic dilutions. Adherence of *E. coli* to endothelial cells was highly dependent on BadA HN23 expression ($P < 0.001$).

Here, even under denaturing conditions, trimers of hybrids 1 to 3 and BadA HN23 were detectable (Fig. 2B). These results confirm earlier observations showing that an exchange of membrane anchor domains of YadA, Hia, Eib, or UspA1 still allowed surface expression of the respective TAAs (20, 38). However, these reports were all focused on TAAs from gammaproteobacteria while the results reported here demonstrate that a domain exchange between TAAs from bacteria belonging to different bacterial subdivisions still enables surface expression of chimeric TAAs. This strongly supports the model of an evolutionary TAA development by domain and subdomain exchange based on the modular construction of these adhesins.

Clearly, BadA HN23 hybrid 3-expressing *E. coli* mimics some biological phenotypes of *B. henselae*. Autoagglutination, collagen binding, and binding to ECs, all originally described to be mediated by BadA in *B. henselae* (4), were transferred to *E. coli*. As these functions are known to be attributed to the head domain of BadA of *B. henselae* (15), the results described here fit our earlier observations. It should be mentioned that we failed to visualize surface expression of BadA HN23 hybrid 3 by electron microscopy (data not shown). However, one should realize that TAA expression has been detected ultrastructurally so far only for BadA of *B. henselae* (4), for the Vomps of *B. quintana* (5), and once for YadA of *Y. enterocolitica* (10).

For analysis of the contribution of BadA HN23 hybrid 3 to EC binding, we had to adjust the experimental approach. The first attempts to analyze the adherence of *E. coli* resulted in massive cell destruction when HUVECs monolayers were infected for 30 min (data not shown). It is known that lipopolysaccharide (LPS) of *E.*

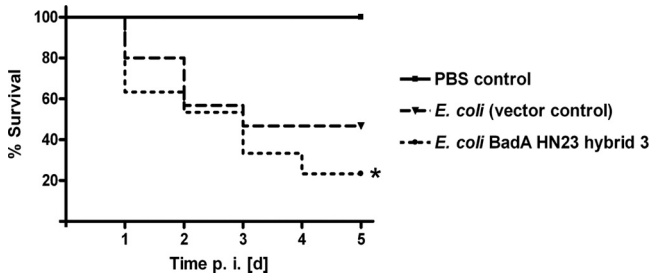

FIG 7 Kaplan-Meier plot of survival after infection with *E. coli* expressing BadA HN23 hybrid 3. *G. mellonella* larvae were infected with *E. coli* BadA HN23 hybrid 3 (resuspended in 10 μl of PBS) at 1.0×10^7 per larva ($n = 30$). Two control groups were included: uninfected *G. mellonella* larvae ($n = 30$) inoculated with sterile PBS (injection control) and *E. coli* (empty vector control; 1.0×10^7)-infected *G. mellonella* larvae ($n = 30$). p.i. [d], days postinfection. *, significant difference in larva survival between vector control and BadA HN23 hybrid 3 ($P < 0.01$). Data represent the cumulative results of three independent experiments.

coli triggers rapid damage and apoptosis in ECs *in vivo* (39) and *in vitro* (40). In contrast, LPS from *B. henselae* is not cytotoxic to ECs (41), which is also reflected by the possibility of long-term cultivation of *B. henselae*-infected ECs (42). These problems were overcome by reducing the infection time with *E. coli* to 15 min, which resulted in intact EC monolayers (data not shown) allowing to analyze adhesive properties of BadA HN23 hybrid 3 reliably in cellular infection models. However, a missing EC apoptosis cannot be expected when mimicking *Bartonella* infection with *E. coli* BadA HN23 hybrid 3, as the antiapoptotic VirB/D4 type IV secretion system apparatus of *B. henselae* is not present in *E. coli* (43). It is also highly unlikely that mechanisms of BadA-mediated angiogenic reprogramming of host cells by *B. henselae* (culminating in the secretion of VEGF 24 h upon infection [2]) can be analyzed in an *E. coli*-based infection model.

G. mellonella has been recently established as an *in vivo* infection model and is of special value when murine infection models are not available (24, 44). Larvae of *G. mellonella* can be kept at 37°C, a temperature at which most human-pathogenic microorganisms have their growth optimum. Moreover, the innate immune system of *G. mellonella* is similar to that of humans and applies to phagocytotic cells (e.g., hemocytes), antimicrobial peptides (e.g., lysozyme), and reactive oxygen species (45). Employing this infection model, expression of BadA HN23 hybrid 3 on the surface of *E. coli* contributed to enhanced *in vivo* pathogenicity. However, the reason for this phenomenon remains unclear. Someone might speculate that bacteria forming aggregates (due to autoagglutination) might be less susceptible to phagocytosis or that attack by antimicrobial peptides can affect only the outer cell layer in such aggregates. Additionally, expression of BadA HN23 hybrid 3 might also enable *E. coli* to adhere to certain insect cells, resulting in infectious damage in the host.

We have not been successful in mimicking some other confirmed biological functions of orthologously expressed BadA HN23 (15, 16). For instance, recombinant BadA HN23 hybrid 3 expression did not confer complement resistance when bacteria were exposed to human serum for 2 h (data not shown). Although complement resistance has been excluded for *B. henselae* in a previous publication (46), it is well known that TAAs (such as YadA [33, 47] or UspA [48]) confer serum resistance. From this, we conclude at least that the membrane anchor of YadA and truncated and hererologously expressed BadA do not contribute to serum resistance. Moreover, we were not successful in detecting the immunodominant characteristics of BadA in *E. coli*. Neither immunofluorescence-based (according to diagnostically accepted algorithms [49]) nor experimental immunoblot-based (50) testing allowed to distinguish reliably between control sera of healthy donors and sera of patients suffering from a *B. henselae* infection (data not shown). The reasons for these differences are currently unclear, and it might be assumed that, e.g., differences in posttranslational modifications of processed and expressed adhesins in *E. coli* or in *B. henselae* might account for such discrepancies.

Taken together, truncated BadA can be recombinantly expressed in *E. coli* by combining TAA domains, and such expression allows the *in vitro* and *in vivo* analysis of biological phenotypes of *B. henselae* in *E. coli*. In particular, such expression strategies might facilitate the exact molecular analysis of domain-function relationships of BadA as they avoid the technical obstacles arising from the slow growth and the difficulties in genetic manipulation of *B. henselae*. Generally, the work described here emphasizes the process of "domain swapping," and this underlines the concept of modular evolution of TAAs.

ACKNOWLEDGMENT

This work was partially funded by a grant from the Bundesministerium für Bildung und Forschung (Leading-Edge Cluster Ci3; FKZ 031A012A) to V.A.J.K.

REFERENCES

1. **Pugh CW, Ratcliffe PJ.** 2003. Regulation of angiogenesis by hypoxia: role of the HIF system. Nat. Med. **9:**677–684. http://dx.doi.org/10.1038/nm0603-677.
2. **Kempf VA, Volkmann B, Schaller M, Sander CA, Alitalo K, Riess T, Autenrieth IB.** 2001. Evidence of a leading role for VEGF in *Bartonella henselae*-induced endothelial cell proliferations. Cell. Microbiol. **3:**623–632. http://dx.doi.org/10.1046/j.1462-5822.2001.00144.x.
3. **Kempf VA, Lebiedziejewski M, Alitalo K, Wälzlein JH, Ehehalt U, Fiebig J, Huber S, Schütt B, Sander CA, Müller S, Grassl G, Yazdi AS, Brehm B, Autenrieth IB.** 2005. Activation of hypoxia-inducible factor-1 in bacillary angiomatosis: evidence for a role of hypoxia-inducible factor-1 in bacterial infections. Circulation **111:**1054–1062. http://dx.doi.org/10.1161/01.CIR.0000155608.07691.B7.
4. **Riess T, Andersson SG, Lupas A, Schaller M, Schäfer A, Kyme P, Martin J, Wälzlein JH, Ehehalt U, Lindroos H, Schirle M, Nordheim A, Autenrieth IB, Kempf VA.** 2004. *Bartonella* adhesin A mediates a proangiogenic host cell response. J. Exp. Med. **200:**1267–1278. http://dx.doi.org/10.1084/jem.20040500.
5. **Müller NF, Kaiser PO, Linke D, Schwarz H, Riess T, Schäfer A, Eble JA, Kempf VA.** 2011. Trimeric autotransporter adhesin-dependent adherence of *Bartonella henselae*, *Bartonella quintana*, and *Yersinia enterocolitica* to matrix components and endothelial cells under static and dynamic flow conditions. Infect. Immun. **79:**2544–2553. http://dx.doi.org/10.1128/IAI.01309-10.
6. **O'Rourke F, Schmidgen T, Kaiser PO, Linke D, Kempf VA.** 2011. Adhesins of *Bartonella* spp. Adv. Exp. Med. Biol. **715:**51–70. http://dx.doi.org/10.1007/978-94-007-0940-9_4.
7. **Leo JC, Goldman A.** 2009. The immunoglobulin-binding Eib proteins from *Escherichia coli* are receptors for IgG Fc. Mol. Immunol. **46:**1860–1866. http://dx.doi.org/10.1016/j.molimm.2009.02.024.
8. **Comanducci M, Bambini S, Brunelli B, Adu-Bobie J, Arico B, Capecchi B, Giuliani MM, Masignani V, Santini L, Savino S, Granoff DM, Caugant DA, Pizza M, Rappuoli R, Mora M.** 2002. NadA, a novel vaccine candidate of *Neisseria meningitidis*. J. Exp. Med. **195:**1445–1454. http://dx.doi.org/10.1084/jem.20020407.
9. **St Geme J, III, Cutter D.** 2000. The *Haemophilus influenzae* Hia adhesin is an autotransporter protein that remains uncleaved at the C terminus and fully cell associated. J. Bacteriol. **182:**6005–6013. http://dx.doi.org/10.1128/JB.182.21.6005-6013.2000.

10. **Hoiczyk E, Roggenkamp A, Reichenbecher M, Lupas A, Heesemann J.** 2000. Structure and sequence analysis of *Yersinia* YadA and *Moraxella* UspAs reveal a novel class of adhesins. EMBO J. **19:**5989–5999. http://dx.doi.org/10.1093/emboj/19.22.5989.
11. **Ray SK, Rajeshwari R, Sharma Y, Sonti RV.** 2002. A high-molecular-weight outer membrane protein of *Xanthomonas oryzae pv. oryzae* exhibits similarity to non-fimbrial adhesins of animal pathogenic bacteria and is required for optimum virulence. Mol. Microbiol. **46:**637–647. http://dx.doi.org/10.1046/j.1365-2958.2002.03188.x.
12. **Linke D, Riess T, Autenrieth IB, Lupas A, Kempf VA.** 2006. Trimeric autotransporter adhesins: variable structure, common function. Trends Microbiol. **14:**264–270. http://dx.doi.org/10.1016/j.tim.2006.04.005.
13. **Szczesny P, Linke D, Ursinus A, Bär K, Schwarz H, Riess TM, Kempf VA, Lupas AN, Martin J, Zeth K.** 2008. Structure of the head of the *Bartonella* adhesin BadA. PLoS Pathog. **4:**e1000119. http://dx.doi.org/10.1371/journal.ppat.1000119.
14. **Riess T, Raddatz G, Linke D, Schäfer A, Kempf VA.** 2007. Analysis of *Bartonella* adhesin A expression reveals differences between various *B. henselae* strains. Infect. Immun. **75:**35–43. http://dx.doi.org/10.1128/IAI.00963-06.
15. **Kaiser PO, Riess T, Wagner CL, Linke D, Lupas AN, Schwarz H, Raddatz G, Schäfer A, Kempf VA.** 2008. The head of *Bartonella* adhesin A is crucial for host cell interaction of *Bartonella henselae*. Cell. Microbiol. **10:**2223–2234. http://dx.doi.org/10.1111/j.1462-5822.2008.01201.x.
16. **Kaiser PO, Linke D, Schwarz H, Leo JC, Kempf VA.** 2012. Analysis of the BadA stalk from *Bartonella henselae* reveals domain-specific and domain-overlapping functions in the host cell infection process. Cell. Microbiol. **14:**198–209. http://dx.doi.org/10.1111/j.1462-5822.2011.01711.x.
17. **Lu YY, Franz B, Truttmann MC, Riess T, Gay-Fraret J, Faustmann M, Kempf VA, Dehio C.** 2013. *Bartonella henselae* trimeric autotransporter adhesin BadA expression interferes with effector translocation by the VirB/D4 type IV secretion system. Cell. Microbiol. **15:**759–778.
18. **Szczesny P, Lupas A.** 2008. Domain annotation of trimeric autotransporter adhesins-daTAA. Bioinformatics **24:**1251–1256. http://dx.doi.org/10.1093/bioinformatics/btn118.
19. **Hartmann MD, Grin I, Dunin-Horkawicz S, Deiss S, Linke D, Lupas AN, Hernandez AB.** 2012. Complete fiber structures of complex trimeric autotransporter adhesins conserved in enterobacteria. Proc. Natl. Acad. Sci. U. S. A. **109:**20907–20912. http://dx.doi.org/10.1073/pnas.1211872110.
20. **Ackermann N, Tiller M, Anding G, Roggenkamp A, Heesemann J.** 2008. Contribution of trimeric autotransporter C-terminal domains of oligomeric coiled-coil adhesin (Oca) family members YadA, UspA1, EibA, and Hia to translocation of the YadA passenger domain and virulence of *Yersinia enterocolitica*. J. Bacteriol. **190:**5031–5043. http://dx.doi.org/10.1128/JB.00161-08.
21. **Laird WJ, Cavanaugh DC.** 1980. Correlation of autoagglutination and virulence of yersiniae. J. Clin. Microbiol. **11:**430–432.
22. **Prilipov A, Phale PS, van Gelder P, Rosenbusch JP, Koebnik R.** 1998. Coupling site-directed mutagenesis with high-level expression: large scale production of mutant porins from *E. coli*. FEMS Microbiol. Lett. **163:**65–72. http://dx.doi.org/10.1111/j.1574-6968.1998.tb13027.x.
23. **Kempf VA, Schaller M, Behrendt S, Volkmann B, Aepfelbacher M, Cakman I, Autenrieth IB.** 2000. Interaction of *Bartonella henselae* with endothelial cells results in rapid bacterial rRNA synthesis and replication. Cell. Microbiol. **2:**431–441. http://dx.doi.org/10.1046/j.1462-5822.2000.00072.x.
24. **Fuchs BB, O'Brien E, Khoury JB, Mylonakis E.** 2010. Methods for using *Galleria mellonella* as a model host to study fungal pathogenesis. Virulence **1:**475–482. http://dx.doi.org/10.4161/viru.1.6.12985.
25. **Zhang P, Chomel BB, Schau MK, Goo JS, Droz S, Kelminson KL, George SS, Lerche NW, Koehler JE.** 2004. A family of variably expressed outer-membrane proteins (Vomp) mediates adhesion and autoaggregation in *Bartonella quintana*. Proc. Natl. Acad. Sci. U. S. A. **101:**13630–13635. http://dx.doi.org/10.1073/pnas.0405284101.
26. **Leo JC, Lyskowski A, Hattula K, Hartmann MD, Schwarz H, Butcher SJ, Linke D, Lupas AN, Goldman A.** 2011. The structure of *E. coli* IgG-binding protein D suggests a general model for bending and binding in trimeric autotransporter adhesins. Structure **19:**1021–1030. http://dx.doi.org/10.1016/j.str.2011.03.021.
27. **Skurnik M, Bolin I, Heikkinen H, Piha S, Wolf-Watz H.** 1984. Virulence plasmid-associated autoagglutination in *Yersinia* spp. J. Bacteriol. **158:**1033–1036.
28. **Alsmark CM, Frank AC, Karlberg EO, Legault BA, Ardell DH, Canback B, Eriksson AS, Naslund AK, Handley SA, Huvet M, La SB, Holmberg M, Andersson SG.** 2004. The louse-borne human pathogen *Bartonella quintana* is a genomic derivative of the zoonotic agent *Bartonella henselae*. Proc. Natl. Acad. Sci. U. S. A. **101:**9716–9721. http://dx.doi.org/10.1073/pnas.0305659101.
29. **Heise T, Dersch P.** 2006. Identification of a domain in *Yersinia virulence* factor YadA that is crucial for extracellular matrix-specific cell adhesion and uptake. Proc. Natl. Acad. Sci. U. S. A. **103:**3375–3380. http://dx.doi.org/10.1073/pnas.0507749103.
30. **Roggenkamp A, Ackermann N, Jacobi CA, Truelzsch K, Hoffmann H, Heesemann J.** 2003. Molecular analysis of transport and oligomerization of the *Yersinia enterocolitica* adhesin YadA. J. Bacteriol. **185:**3735–3744. http://dx.doi.org/10.1128/JB.185.13.3735-3744.2003.
31. **Roggenkamp A, Neuberger HR, Flügel A, Schmoll T, Heesemann J.** 1995. Substitution of two histidine residues in YadA protein of *Yersinia enterocolitica* abrogates collagen binding, cell adherence and mouse virulence. Mol. Microbiol. **16:**1207–1219. http://dx.doi.org/10.1111/j.1365-2958.1995.tb02343.x.
32. **Tahir YE, Kuusela P, Skurnik M.** 2000. Functional mapping of the *Yersinia enterocolitica* adhesin YadA. Identification of eight NSVAIG - S motifs in the amino-terminal half of the protein involved in collagen binding. Mol. Microbiol. **37:**192–206. http://dx.doi.org/10.1046/j.1365-2958.2000.01992.x.
33. **Schindler MK, Schütz MS, Mühlenkamp MC, Rooijakkers SH, Hallström T, Zipfel PF, Autenrieth IB.** 2012. *Yersinia enterocolitica* YadA mediates complement evasion by recruitment and inactivation of C3 products. J. Immunol. **189:**4900–4908. http://dx.doi.org/10.4049/jimmunol.1201383.
34. **Journet L, Agrain C, Broz P, Cornelis GR.** 2003. The needle length of bacterial injectisomes is determined by a molecular ruler. Science **302:**1757–1760. http://dx.doi.org/10.1126/science.1091422.
35. **Lehr U, Schütz M, Oberhettinger P, Ruiz-Perez F, Donald JW, Palmer T, Linke D, Henderson IR, Autenrieth IB.** 2010. C-terminal amino acid residues of the trimeric autotransporter adhesin YadA of *Yersinia enterocolitica* are decisive for its recognition and assembly by BamA. Mol. Microbiol. **78:**932–946. http://dx.doi.org/10.1111/j.1365-2958.2010.07377.x.
36. **Arnold T, Zeth K, Linke D.** 2010. Omp85 from the thermophilic cyanobacterium *Thermosynechococcus elongatus* differs from proteobacterial Omp85 in structure and domain composition. J. Biol. Chem. **285:**18003–18015. http://dx.doi.org/10.1074/jbc.M110.112516.
37. **Paramasivam N, Habeck M, Linke D.** 2012. Is the C-terminal insertional signal in Gram-negative bacterial outer membrane proteins species-specific or not? BMC Genomics **13:**510. http://dx.doi.org/10.1186/1471-2164-13-510.
38. **Mikula KM, Leo JC, Lyskowski A, Kedracka-Krok S, Pirog A, Goldman A.** 2012. The translocation domain in trimeric autotransporter adhesins is necessary and sufficient for trimerization and autotransportation. J. Bacteriol. **194:**827–838. http://dx.doi.org/10.1128/JB.05322-11.
39. **McGrath JM, Stewart GJ.** 1969. The effects of endotoxin on vascular endothelium. J. Exp. Med. **129:**833–848. http://dx.doi.org/10.1084/jem.129.5.833.
40. **Shioiri T, Muroi M, Hatao F, Nishida M, Ogawa T, Mimura Y, Seto Y, Kaminishi M, Tanamoto K.** 2009. Caspase-3 is activated and rapidly released from human umbilical vein endothelial cells in response to lipopolysaccharide. Biochim. Biophys. Acta **1792:**1011–1018. http://dx.doi.org/10.1016/j.bbadis.2009.06.006.
41. **Zähringer U, Lindner B, Knirel YA, Van Den Akker WM, Hiestand R, Heine H, Dehio C.** 2004. Structure and biological activity of the short-chain lipopolysaccharide from *Bartonella henselae* ATCC 49882T. J. Biol. Chem. **279:**21046–21054. http://dx.doi.org/10.1074/jbc.M313370200.
42. **Kyme PA, Haas A, Schaller M, Peschel A, Iredell J, Kempf VA.** 2005. Unusual trafficking pattern of *Bartonella henselae*-containing vacuoles in macrophages and endothelial cells. Cell. Microbiol. **7:**1019–1034. http://dx.doi.org/10.1111/j.1462-5822.2005.00531.x.
43. **Schmid MC, Schülein R, Dehio M, Denecker G, Carena I, Dehio C.** 2004. The VirB type IV secretion system of *Bartonella henselae* mediates invasion, proinflammatory activation and antiapoptotic protection of endothelial cells. Mol. Microbiol. **52:**81–92. http://dx.doi.org/10.1111/j.1365-2958.2003.03964.x.
44. **Insua JL, Llobet E, Moranta D, Perez-Gutierrez C, Tomas A, Garmendia J, Bengoechea JA.** 2013. Modeling *Klebsiella pneumoniae* pathogenesis by infection of the wax moth *Galleria mellonella*. Infect. Immun. **81:**3552–3565. http://dx.doi.org/10.1128/IAI.00391-13.
45. **Mukherjee K, Altincicek B, Hain T, Domann E, Vilcinskas A,**

Chakraborty T. 2010. *Galleria mellonella* as a model system for studying *Listeria* pathogenesis. Appl. Environ. Microbiol. **76:**310–317. http://dx.doi.org/10.1128/AEM.01301-09.
46. **Rodriguez-Barradas MC, Bandres JC, Hamill RJ, Trial J, Clarridge JE, III, Baughn RE, Rossen RD.** 1995. *In vitro* evaluation of the role of humoral immunity against *Bartonella henselae*. Infect. Immun. **63:**2367–2370.
47. **Balligand G, Laroche Y, Cornelis G.** 1985. Genetic analysis of virulence plasmid from a serogroup 9 *Yersinia enterocolitica* strain: role of outer membrane protein P1 in resistance to human serum and autoagglutination. Infect. Immun. **48:**782–786.
48. **Singh B, Blom AM, Unal C, Nilson B, Morgelin M, Riesbeck K.** 2010. Vitronectin binds to the head region of *Moraxella catarrhalis* ubiquitous surface protein A2 and confers complement-inhibitory activity. Mol. Microbiol. **75:**1426–1444. http://dx.doi.org/10.1111/j.1365-2958.2010.07066.x.
49. **Centers for Disease Control and Prevention.** 1999. Serodiagnosis of emerging infectious diseases: *Bartonella* and *Ehrlichia* infections (course manual). Centers for Disease Control and Prevention, Atlanta, GA.
50. **Wagner CL, Riess T, Linke D, Eberhardt C, Schäfer A, Reutter S, Maggi RG, Kempf VA.** 2008. Use of *Bartonella* adhesin A (BadA) immunoblotting in the serodiagnosis of *Bartonella henselae* infections. Int. J. Med. Microbiol. **298:**579–590. http://dx.doi.org/10.1016/j.ijmm.2008.01.013.
51. **Drancourt M, Birtles R, Chaumentin G, Vandenesch F, Etienne J, Raoult D.** 1996. New serotype of *Bartonella henselae* in endocarditis and cat-scratch disease. Lancet **347:**441–443. http://dx.doi.org/10.1016/S0140-6736(96)90012-4.
52. **Grosskinsky U, Schütz M, Fritz M, Schmid Y, Lamparter MC, Szczesny P, Lupas AN, Autenrieth IB, Linke D.** 2007. A conserved glycine residue of trimeric autotransporter domains plays a key role in *Yersinia* adhesin A autotransport. J. Bacteriol. **189:**9011–9019. http://dx.doi.org/10.1128/JB.00985-07.